

Author's Accepted Manuscript

An hybrid real genetic algorithm to detect structural damage using modal properties

V. Meruane, W. Heylen

PII: S0888-3270(10)00423-1
DOI: doi:10.1016/j.ymsp.2010.11.020
Reference: YMSSP 2703

To appear in: *Mechanical Systems and Signal*

Received date: 11 August 2008
Revised date: 7 July 2009
Accepted date: 30 November 2010

Cite this article as: V. Meruane and W. Heylen, An hybrid real genetic algorithm to detect structural damage using modal properties, *Mechanical Systems and Signal*, doi:10.1016/j.ymsp.2010.11.020

This is a PDF file of an unedited manuscript that has been accepted for publication. As a service to our customers we are providing this early version of the manuscript. The manuscript will undergo copyediting, typesetting, and review of the resulting galley proof before it is published in its final citable form. Please note that during the production process errors may be discovered which could affect the content, and all legal disclaimers that apply to the journal pertain.



www.elsevier.com/locate/ymsp

An Hybrid Real Genetic Algorithm to Detect Structural Damage Using Modal Properties

V. Meruane^a and W. Heylen^b

^a*Department of Mechanical Engineering, Universidad de Chile.*

*Department of Mechanical Engineering, K.U.Leuven. Celestijnenlaan 300B - bus
2420, B-3001 Heverlee, Belgium.*

^b*Department of Mechanical Engineering, K.U.Leuven. Celestijnenlaan 300B - bus
2420, B-3001 Heverlee, Belgium.*

Abstract

An hybrid real coded Genetic Algorithm with damage penalization is implemented to locate and quantify structural damage. Genetic Algorithms provide a powerful tool to solved optimization problems. With an appropriate selection of their operators and parameters they can potentially explore the entire solution space and reach the global optimum. Here, the set-up of the Genetic Algorithm operators and parameters is addressed, providing guidelines to their selection in similar damage detection problems. The performance of five fundamental functions based on modal data is studied. In addition, this paper proposes the use of a damage penalization that satisfactorily avoids false damage detection due to experimental noise or numerical errors. A tridimensional space frame structure with single and multiple damages scenarios provides an experimental framework which verifies the approach. The method is tested with different levels of incompleteness in the measured degrees of freedom. The results show that this approach reaches a much more precise solution than conventional optimization methods. A scenario of three simultaneous damage locations was correctly located and quantified by measuring only a 6.3% of the total degrees of freedom.

Key words: Damage Detection, Genetic Algorithm, Modal Analysis, Damage Penalization

Email addresses: vmeruane@ing.uchile.cl (V. Meruane),

1 **1 Introduction**

2 The early detection of structural damage generates a wide interest in the
3 civil, mechanical and aerospace engineering fields. Many recent studies focus
4 on the application of vibration-based damage detection methods. While visual
5 inspection fails to assess damage at early stages, vibration measurements are
6 sensitive enough to detect damage even if it is located in hidden or internal
7 areas.

8 Damage detection methods are classified according to the level of identification
9 attempted [1]:

10 **Level 1:** Detecting the presence of damage in the structure;

11 **Level 2:** Determining the geometric location of the damage;

12 **Level 3:** Quantifying the severity of the damage;

13 **Level 4:** Predicting the remaining lifespan.

14 Levels 3 and 4 are the most challenging areas of damage detection, to achieve
15 these levels model-based methods are necessary. These methods correlate a
16 numerical model with measured data from the structure. A set of variables is
17 updated to obtain the minimum difference between the numerical and exper-
18 imental data. Damage is modelled as a reduction of stiffness in an element,
19 and it is detected by comparing the undamaged and damage state.

20 A proper selection of the objective function is crucial since it not only modifies
21 the interpretation of the best correlation, but also influences the convergence
22 of the optimization procedure. Several objective functions have been reported

Ward.Heylen@mech.kuleuven.be (W. Heylen).

23 in the damage detection field. Salawu [2] presents a review of damage detection
24 methods through changes in frequencies. Despite the fact that he emphasizes
25 that damage detection using only natural frequencies is attractive, since it is
26 fast and economical, he concludes that it is not possible to locate and quantify
27 correctly any damage situation by using only frequencies. Hence mode shape
28 data is also necessary.

29 Many authors discuss the problem of detecting damage using mode shapes
30 and frequencies. Shi et al. [3] present a sensitivity based method to locate and
31 quantify damage. Damage is located using incomplete measured modes and
32 it is quantified using the measured natural frequencies. The method is able
33 to detect the real damage but a significant amount of false damage is also
34 detected. Araujo dos Santos et al. [4] propose a damage detection algorithm
35 based on the orthogonality condition sensitivities, their method produces more
36 accurate results than the mode shape sensitivities method. The same method
37 is implemented later by Ren and De Roeck [5, 6]. Wahab [7] studies the effect
38 of including the modal curvatures in the convergence of a sensitivity based
39 method. He concludes that the addition of modal curvatures does not improve
40 the algorithm convergence. Görl and Link [8] implement a damage detection
41 algorithm based on modes and frequencies sensitivities. Although damage is
42 successfully located and quantified, a careful selection of the regularization
43 parameters is necessary to achieve satisfactory results.

44 Other objective functions that make use of modal data are strain energy,
45 modal flexibility and residual forces. A disadvantage of these functions is that
46 they need a sufficient fine spatial resolution. Jaishi and Ren [9] update the
47 finite element models of a simulated beam and a real bridge using the strain
48 energy residual. Jaishi and Ren [10] implement a sensitivity based algorithm

49 using modal flexibility residuals. The method is verified on simulated and
50 experimental multi-cracked beams. A sensitivity method based on residual
51 forces is implemented by Kosmatka and Ricles [11]. The method is used to
52 detect damage on an experimental space truss structure.

53 The use of the Frequency Response Function (FRF) is also an alternative
54 [12, 13]. The advantage is that no modal extraction is necessary, thus contam-
55 ination of the data with modal extraction errors is avoided. However, complex
56 FRF data with noise can make the convergence process very slow and often
57 numerically unstable as was found by Imregun et al. [[13]. Furthermore, the
58 success of the method is highly dependent on the selection of the frequency
59 points. Lammens [14] addresses how a poor selection of the frequency points
60 can lead to an unstable updating process and inaccurate results. FRFs have
61 also the disadvantage that they can not be identified from output only modal
62 analysis with ambient excitation, thus the excitation by an artificial force is
63 always required.

64 Conventional optimization techniques used in damage detection or model up-
65 dating employ sensitivity based searching mechanisms. These searching mech-
66 anisms do not assure to reach an unique optimum solution because they are
67 highly sensitive to the initial searching conditions and they usually lead to lo-
68 cal minima. Moreover, the ill-conditioned inverse problem leads to instabilities
69 and the convergence is not always assured. According to Natke [15] the only
70 solution to overcome ill-conditioning is the regularization of the equations.
71 However, the regularization parameters must be carefully selected, since the
72 speed of convergence and the quality of the results strongly depends on them
73 [16]. It seems, therefore, that further investigations are needed to implement a
74 robust optimization approach to deal with these problems. Since John Holland

75 first developed the genetic algorithm (GA) in 1975, it has been increasingly in-
76 troduced in diverse areas such as music generation, genetic synthesis, strategy
77 planning, machine learning and damage detection [17].

78 The GA is a global searching process based on the Darwin's principle of nat-
79 ural selection and evolution. A simple GA consists in three main operations:
80 selection, genetic operations and replacement. The GA starts with an initial
81 population; the individuals of this population are subjected to the three op-
82 erators and evolve. The result is a population with a higher fitness than the
83 initial one as in natural selection. This process is iterated for a number of
84 generations until a convergence criterion is achieved. There are three main
85 selection processes: roulette wheel [18], normalized geometric [19] and tourna-
86 ment selection [20]. To increase the speed of convergence an elitist strategy can
87 be adopted. Crossover and mutation are applied randomly with a probability
88 of p_c and p_m respectively. The crossover is considered the main search oper-
89 ator in GAs, as a consequence many types of crossover have been developed.
90 Some of them are: single point crossover, two point crossover [21], uniform
91 crossover [22], flat crossover [23], arithmetic crossover [24], heuristic crossover
92 [25], blend crossover [26], BLX- crossover [26], and many more. The mutation
93 operation replaces a gene in a chromosome with one chosen randomly from the
94 solution space. In uniform mutation the gene is set equal to a uniform random
95 number, and in boundary mutation it is set equal to either its lower or upper
96 bound. A correct selection of the GA operators and parameters is crucial as
97 they affect the solution and the algorithm runtime [27]. However, there is no
98 general rule to select them; the right decision depends on the number of genes,
99 the objective function and the nature of the problem. This paper studies the
100 problem of selecting the GA operators and parameters during the implementa-

101 tion of a structural damage detection algorithm. This results in guidelines for
102 GA operator and parameter selection in similar damage detection problems.

103 Binary-coded genetic algorithms (BCGA) were the first GA-methods to be in-
104 troduced in damage detection [28–33]. Recently, there has been growing inter-
105 est on implementing real-coded genetic algorithms (RCGA) [34–37], since they
106 work better with continuous variables and require less storage than BCGA.
107 RCGA are inherently faster since decoding the binary variables before each
108 evaluation is not necessary. In addition RCGA do not have a limited preci-
109 sion as do BCGA; this allows a representation to the machine precision [38].
110 Although RCGAs have already been implemented in damage detection al-
111 gorithm, they are modern techniques that are still under development. As a
112 consequence, there are still problems to be investigated regarding to their im-
113 plementation, such as: environmental effect, experimental noise, selection of
114 the objective function, selection of adequate GA parameters and operators,
115 parallelization and hybridization ... [39].

116 The performance of BCGA and RCGA in the crack detection of a cantilever
117 beam is studied by Vakil-Baghmisheh et al. [36]. A numerical model of a beam
118 with a single crack is proposed. Numerical and experimental data is used to
119 test the performance. The best average values of location and deep prediction
120 are obtained with the RCGA. Gomes and Silva [37] compared the perfor-
121 mance of a RCGA and a sensitivity method for damage detection. They use
122 only natural frequencies in the objective function. The method is tested with
123 noise free simulated data of a simple supported beam and a portal frame. No
124 general conclusions are obtained from the results, since both methods have
125 problems in locating and evaluating the extension of the damage. To improve
126 their results also mode shapes should have been considered, it has already been

127 demonstrated that with only natural frequencies it is not possible to locate and
128 quantified any damage situation [2]. A BCGA with residual forces is imple-
129 mented by Mares and Surace [28] to detect structural damage. The method is
130 tested with simulated data of a five-bay truss structure and a cantilever beam.
131 Rao et al. [29] also work with force residuals and BCGA optimization to de-
132 tect damage of simulated truss structures. Ruotolo and Surace [30] describe a
133 damage detection of a multiple cracked beam with both simulated and exper-
134 imental data. The problem is solved with a BCGA using three fundamentals
135 objective functions based on natural frequencies, modal displacements and
136 modal curvatures. Chou and Ghanboussi [31] use simulated measurements
137 of static displacements and a BCGA to detect damage in two plane truss
138 structures. Asce and Xia [34] implement a damage detection algorithm us-
139 ing a RCGA to minimize an objective function based on natural frequencies
140 and mode shapes. The algorithm is evaluated with an experimental cantilever
141 beam and an experimental portal frame. An algorithm that combines RCGA
142 and simulated annealing is proposed by He and Hwang [35] to detect dam-
143 age in beam-types structures. A modified GA is developed by Borges et al.
144 [40] to detect damage in framed structures. They proposed: discrete values to
145 represent the damage, a heuristic generation of the initial population, two dy-
146 namically varying fitness functions based on modal data and two specialized
147 mutation operators. Kouchmeshky et al. [41, 42] proposed a two stages algo-
148 rithm to detect structural damage. First the algorithm searches for possible
149 damage scenarios and secondly the algorithm searches for tests that incre-
150 ment the level of information, in both stages GA are used. The feasibility
151 of the method is demonstrated in several examples with simulated data of a
152 four-span bridge truss. This methodology is useful in cases where only a few
153 measurements can be obtained on each test. Perera et at. [33] compared four

154 multiobjective algorithms based on a BCGA for the application of structural
155 damage identification. Two objective functions are considered, the first based
156 on the modal flexibility and the second based on modes and frequencies. The
157 method is tested with numerical and experimental data of a simply supported
158 beam. The best results are obtained with the strength pareto evolutionary
159 algorithm, although considerable false damage is detected.

160 Genetic Algorithms are inherently slow when they work with complicated or
161 time consuming objective functions. This is partly solved by combining the
162 power of GA with the speed of a local optimizer (hybrid-GA). Thus, the GA
163 finds the regions of the optimum, and the local optimizer finds the minimum.
164 Friswell et al. [31] solve the damage detection problem in two stages. First,
165 the damage is located with a BCGA, and second the eigensensitivity method
166 is used to quantify the damage extend. The method is verified with a simu-
167 lated cantilever beam and an experimental steel plate. Koh et al. [32] identify
168 damage on a large structure using a hybrid optimization approach. The opti-
169 mization is handled with a BCGA followed with a least square optimization.
170 Au et al. [43] work with a two step procedure; first the element quotient dif-
171 ference is employed to locate the damage and second a micro-GA is used to
172 quantify it. Simulated beams with multiple damage are use to verified the
173 approach. Raich et al. [44] studied the performance of an hybrid GA in de-
174 tecting damage of a cantilever beam, a two-span beam and a steel frame, in
175 the three cases simulated noisy data is used. The performance is evaluated
176 for a fixed representation and an implicit redundant representation, the GA
177 search is followed by local search algorithm to improve the solution accuracy.
178 They concluded that an implicit redundant representation provides a greater
179 accuracy in detecting and locating damage.

180 Most of the papers cited here focus on finding a robust optimization proce-
181 dure that reaches the global optimum using an objective function that is sen-
182 sitive enough to structural damage. However, little attention has been paid to
183 minimizing the effect of experimental noise or numerical errors in the damage
184 detection procedure. Experimental noise and numerical errors generate differ-
185 ences between the numerical and experimental data that can be interpreted
186 as damage. This false damage causes a minor improvement in the correlation;
187 consequently, a significant amount of false damage can be detected. Ruotolo
188 and Surace [30] introduce a weighting term in the objective function to pro-
189 mote the location of damage at fewer sites. With the introduction of this term,
190 false damage detection was significantly reduced. Friswell et al. [31] add a pe-
191 nalization term in the objective function when there is more than one damage
192 location detected. This penalization works fine when there is only one damage
193 location, but is not intended for multiple damages. Xia et al. [45] study the
194 effect of experimental and numerical noise on false damage detection. They
195 implement a statistical method to define the probability of damage existence.

196 The present study implements a hybrid-RCGA to detect structural damage. It
197 addresses the set-up of the GA parameters and operators. It studies different
198 objective functions, which are based on frequencies, mode shapes, strain energy
199 and modal flexibility. The chosen objective function is the one that provides
200 both the best convergence and solution. Additionally, the paper proposes a
201 damage penalization term that successfully avoids the problem of false damage
202 detection because of experimental noise or numerical errors. A tridimensional
203 space frame structure with single and multiple damages scenarios provides an
204 experimental framework which verifies the approach. The results are compared
205 with those obtained through conventional methods such as the Inverse Eigen-

206 Sensitivity Method and the Response Function Method. The accuracy of the
 207 method is tested with different levels of incompleteness in the measured data.

208 **2 Damage Detection Procedure**

209 The damage is represented by an elemental stiffness reduction factor β_i , de-
 210 fined as the ratio of the stiffness reduction to the initial stiffness. The stiffness
 211 matrix of the damage structure $[K_d]$ is expressed as a sum of element matrices
 212 multiplied by reduction factors,

$$[K_d] = \sum_i (1 - \beta_i) [K_i] \quad (1)$$

213 The value $\beta_i = 0$ indicates that the element is undamaged whereas $0 < \beta_i \leq 1$
 214 implies partial or complete damage. This is the simplest method to model
 215 damage. Although this model has problems in matching damage severity to
 216 crack depth and is affected by mesh density, Friswell and Penny [46] demon-
 217 strated that at low frequencies this method can correctly model a crack. It was
 218 shown that a more detailed model does not substantially improve the results
 219 from damage assessment

220 The problem of detecting damage is a constrained nonlinear optimization
 221 problem, where the damage reduction factors of each beam β_i are defined
 222 as updating parameters. An objective function represents the error between
 223 the measured and numerical modal data. To assess the more efficient objective
 224 function, five fundamental objective functions have been considered,

(1) The error in frequency,

$$F_1(\{\beta\}) = \sum_i \left(\frac{\lambda_{A,i}(\{\beta\})}{\lambda_{E,i}} - 1 \right)^2 = \sum_i \left(\frac{\omega_{A,i}^2(\{\beta\})}{\omega_{E,i}^2} - 1 \right)^2 \quad (2)$$

225 The subscripts A and E refer to analytical and experimental respectively. λ_i
226 is the i th eigenvalue and ω_i is the i th natural frequency.

(2) The modal displacements difference,

$$F_2(\{\beta\}) = \sum_i \|\{\phi_{A,i}\} - \{\phi_{E,i}\}\|^2 \quad (3)$$

227 Where ϕ_i is the i th mode shape. This difference is evaluated only at the
228 measured degrees of freedom. Equation 3 can only be applied if both sets
229 of mode shapes are consistently normalized. Experimental modes shapes
230 are normalized using the modal scale factor MSF [47].

(3) The MAC value,

$$F_3(\{\beta\}) = \sum_i (1 - MAC(\{\phi_{A,i}\}, \{\phi_{E,i}\}))^2 \quad (4)$$

231 MAC [47] is a factor that expresses the correlation between two modes.
232 A value of 0 indicates no correlation, whereas a value of 1 indicates two
233 completely correlated modes. Scaling of the modes is not required here
234 and the MAC value can be computed using only the measured degrees of
235 freedom.

(4) The strain energy residual [9],

$$F_4(\{\beta\}) = \sum_i \left(\frac{\{\phi_{A,i}\}^T [K] \{\phi_{A,i}\}}{\{\phi_{E,i}\}^T [K] \{\phi_{E,i}\}} - 1 \right)^2 \quad (5)$$

236 $[K]$ is the analytical stiffness matrix. The normalization of both the an-

237 analytical and experimental mode shapes must be consistent. Expansion of
 238 the measured mode shapes and/or reduction of the numerical model is
 239 needed to match the experimental and analytical degrees of freedom.

(5) The difference between experimental and analytical modal flexibility matrices [10],

$$F_5(\{\beta\}) = \left\| [\Phi_A] [\Lambda_A] [\Phi_A]^T - [\Phi_E] [\Lambda_E] [\Phi_E]^T \right\|^2 \quad (6)$$

240 Where $[\Phi]$ is the eigenvector matrix and $[\Lambda]$ is the eigenvalue matrix.
 241 Analytical and experimental modes shapes must be properly scaled. The
 242 modal flexibility can be estimated using only the measured degrees of
 243 freedom [10].

244 The objective function J considers some of these five fundamental functions
 245 plus a damage penalization term,

$$J(\{\beta\}) = \sum_{j=1}^5 \delta_j \frac{F_j(\{\beta\})}{F_{j,0}} + \gamma \sum_i \beta_i \quad (7)$$

246 $F_{j,0}$ refers to the initial values of $F_j(\beta = 0)$, δ_j equals to 1 if the error func-
 247 tion F_j is considered and 0 if not. By adding the damage penalization term
 248 $\gamma \sum_i \beta_i$, the objective function searches not only for the best correlation, but
 249 also the minimum possible damage. Thus, avoiding false damage detection
 250 because of experimental noise or numerical errors. The value of γ depends on
 251 the confidence in the numerical model and the experimental data. Although
 252 a similar damage penalization was proposed by Ruotolo and Surace [30] in
 253 1997 obtaining a significance reduction of the false damage detected, no later
 254 references to this penalization have been found.

255 The optimization problem is defined as,

$$\begin{aligned}
 & \min && J(\{\beta\}) \\
 & \text{subject to} && F_j(\{\beta\}) \leq F_{j,0} \\
 & && 0 \leq \beta_i \leq 1
 \end{aligned} \tag{8}$$

256 The aim is to minimize the objective function J , but GA always maximizes
 257 a problem. The minimization problem is transformed into a maximization
 258 problem by defining the objective function as a suitable number subtracted
 259 by J .

260 3 Application Case

261 Figure 1 shows the experimental setup, the structure is a tridimensional stat-
 262 ically indeterminate space truss, consisting of 43 members and 20 joins. This
 263 configuration has been chosen for the following reasons: First, it provides a
 264 reasonable number of global and local modes. Second, it presents a balanced
 265 combination of well separated and close modes. Third, it has nodes connecting
 266 several elements, which makes the damage identification process [41, 42] more
 267 difficult. The dimensions of the structure are: length: $3m$, width: $0.5m$, height:
 268 $0.5m$. Each beam has a diameter of $20mm$. The structure is suspended by soft
 269 springs to simulate a “free-free” boundary condition.

270 The Finite Element Model was built on Matlab using $3D$ truss elements for
 271 the bars and concentrated inertia elements for the joins. Each bar is modeled

272 with four truss elements as shown in Figure 2. Rotational degrees of freedom
273 were deleted from the FE model using the Guyan reduction technique [48]. As
274 a result, the model has a total of 447 degrees of freedom and 192 elements.
275 A total of 12 global modes are computed with frequencies between $12Hz$ and
276 $125Hz$, subsequent modes are local bar modes. Damage is considered at the
277 bar level, so all elements on each bar are grouped in a single macro-element.

278 The optimum response configuration is determined by minimizing the MAC
279 off-diagonal values [49]. Thus all the measured modes are independent between
280 each other. For visual representation purposes, all nodes are instrumented with
281 tri-axial accelerometers. As a consequence, a total of 20×3 degrees of freedom
282 are measured; one tri-axial accelerometer per join.

283 The selection of the excitation and suspension locations is based on the study
284 of the driving point residues (DPR) [50]. The DPR with large values for as
285 many modes as possible indicate good excitation points. In addition, the DPR
286 with lower values indicate good suspension locations.

287 The frequency range of analysis covers the range from 0 to $256 Hz$ with a
288 resolution of $0.25Hz$. This range contains all global modes and also a list of
289 local modes. Figure 3 presents the correlation between the numerical and ex-
290 perimental modes in the undamaged state. The maximum frequency difference
291 is 2.3% and the minimum MAC value is 0.86.

292 *3.1 Damage Introduction*

293 Four damage cases are studied. In the first three cases, a few aluminum bars
294 are replaced by plastic bars, thus the stiffness and mass of the replaced bar is

295 reduced. The replaced bars on each case are: **case 1**: bar 6; **case 2**: bars 6
 296 and 25; **case 3**: bars 6, 25 and 43. In **case 4** bar 34 was completely removed
 297 from the structure. Figure 4 shows the bar numbering.

298 Figure 5 shows the correlation between the undamaged numerical modes and
 299 the damaged experimental modes. In the first case, a new mode is detected
 300 at $139Hz$. It is also possible to see a considerable decrease in the correlation
 301 of modes 10 and 11. In the second case, a new mode is detected at $135Hz$. In
 302 addition, the correlation of modes 10 and 11 is reduced, and the frequency of
 303 mode 12 is reduced by 35%. In case 3, two new modes are detected at $135Hz$
 304 and $143Hz$, the correlation of modes 10 and 11 is considerable reduced, and
 305 the frequency of mode 12 is reduced by 40%. In case 4 there is a swap of modes
 306 5 and 6, a new mode is detected at $46.7Hz$ and the correlation of mode 11 is
 307 reduced.

308 4 Methodology

309 4.1 Objective Function

310 To correctly model the experimental damage, i.e., replacing or removing a
 311 bar, a mass reduction factor ρ_i must also be considered. For convenience the
 312 mass reduction factor is defined proportional to the stiffness reduction factor,
 313 this allows to update only the stiffness parameters as in a general damage
 314 detection algorithm,

$$\rho_i = \alpha \cdot \beta_i \quad (9)$$

315 The ratio of the stiffness reduction to the mass reduction (α) was experimen-
316 tally determined. When an aluminum bar is replaced by a plastic bar α equals
317 0.73, whereas when a bar is removed α equals 1.

318 Five objective functions were evaluated, the one that provided the best per-
319 formance was chosen. The objective functions are: (1) frequencies, (2) modes
320 and frequencies, (3) MAC and frequencies, (4) strain energy and frequencies
321 and (5) modal flexibility. The first damage case is used to test the different
322 objective functions. The optimization process is performed with the Genetic
323 Algorithm described in section 4.2. To assess the probability that the algo-
324 rithm would converge to the same solution, each case was run five times during
325 500 generations. Figure 6 presents the convergence curves and the damage de-
326 tected for each objective function and run. The left graphs show the evolution
327 of the objective function (J) evaluated for the fitter member of the population.
328 Each objective function is normalized with its global optimum value J_{opt} . On
329 the right a stacked bar plot shows the damage detected at each run with a
330 different color, an arrow indicates the position of the actual damage. By using
331 only frequencies it is difficult to reach the optimum solution, only two of the
332 five runs could reach the optimum in the desired number of generations. This
333 is because the objective function has several local minimums. These local so-
334 lutions dominate the population and the algorithm relies mainly on mutation
335 which is a slow process. As a consequence, a higher number of generations
336 would be necessary to reach optimum. This problem is partly solved when the
337 modal displacements are added. Here, four of the five runs reach the optimum.
338 The same result is obtained with the modal flexibility. On the other hand, with
339 strain energy and frequencies it was possible to reach the optimum solution in
340 all five runs, but the optimum damage detected does not correspond with the

341 actual damage. Only the objective function MAC and frequencies was able to
342 detect five times the actual damage in the desired number of generations.

343 The value of the penalization weight was delimited after a sensitivity analysis.
344 The results of this analysis are shown in Figure 7. For values of γ between
345 0.08 and 2.5 real damage is successfully detected and false damage is avoided.
346 If γ is lower than 0.08 false damage is detected whereas if γ is greater than
347 2.5 no damage is detected. It should be noticed that the correct values of
348 gamma depend on the structure, level of experimental noise and the errors
349 in the numerical model. Hence, the selected range of gamma is only valid for
350 this particular study case. In other cases a similar sensitivity analysis must be
351 performed.

352 4.2 Genetic Algorithm

353 Each chromosome consists of 43 genes. Each gene is the stiffness reduction
354 factor of a beam element. Each chromosome represents one possible damage
355 distribution; the initial population is generated randomly with real numbers
356 between 0 and 1.

357 Correct selection of the GA operators and parameters is crucial as they affect
358 the solution and the algorithm runtime [27]. However, there is no general rule
359 to select them; the right decision depends on the number of genes, the objective
360 function and the nature of the problem. Here the parameters and operators
361 were selected by optimizing the runtime, i.e., by minimizing the number of
362 function evaluations.

363 Three selection processes were tested: (1) roulette wheel, (2) normalized ge-

364 ometric and (3) tournament selection. In normalized geometric selection the
365 probability of selecting the best was set to 0.08 and in tournament selection
366 the number of individuals on each tournament was set to two. Figure 8 shows
367 the average convergence curve obtained after running 20 times the algorithm
368 with each selection. The normalized geometric selection gives the best con-
369 vergence. Once the selection was set, two mutation operators were evaluated:
370 (1) uniform mutation and (2) boundary mutation. Figure 8 shows the aver-
371 age convergence curves: boundary mutation gives the best performance. The
372 last operator is crossover; here five kinds of crossover were studied: (1) single
373 point crossover, (2) double point crossover, (3) uniform crossover, (4) arith-
374 metic crossover (5) heuristic crossover. Arithmetic crossover yields the best
375 performance, as is shown in Figure 8.

376 Once the GA operators are selected, the method was evaluated with various
377 combinations of mutation and crossover probabilities. For each combination
378 the algorithm was run 20 times, the combination that reached the best average
379 value of the objective function was selected. As is shown in Figure 9 the lowest
380 value of the objective function was reached with a mutation probability of 0.01
381 and a crossover probability of 0.72. The same procedure was followed to select
382 the population size. The best performance was obtained with a population
383 size of 25 as is shown in Figure 9 .

384 Hence the best combination of operators and parameters is: normalized geo-
385 metric selection, arithmetic crossover, boundary mutation, and the following
386 three parameters: population size of 25, $p_m = 0.01$ and $p_c = 0.72$.

387 4.3 Hybrid GA

388 The combination of GA's and a local optimizer makes it possible to reach a
389 high level of accuracy in a moderate computational time. In order to reach
390 the same level of accuracy only with GA's, much more generations would
391 be required. Figure 10 illustrates the curve of convergence obtained with a
392 hybrid-GA. The differences in the damage detected using only GA and with
393 hybrid-GA are also given in Figure 10. The Matlab function *fmincon* was
394 used as a local optimizer. Figure 10 shows that the GA finds the damage
395 locations and a close approximation of their quantity. Then, *fmincon* starts
396 with the solution given by GA and increases the precision.

397 5 Results

398 The damage pattern is obtained through the same procedure on each damage
399 case. The first 12 global modes are used in the objective function. The objec-
400 tive function is based on the frequencies difference and MAC values, including
401 a damage penalization term with a γ value of 0.1. A hybrid-RCGA is used as
402 optimization algorithm. The results are compared with those obtained with
403 two sensitivity based methods, namely, Response Function Method (RFM)
404 and Inverse Eigen-Sensitivity Method (IESM). A description of both methods
405 is found in the paper of Modak et al. [51]. The IESM minimizes the differ-
406 ence between analytical and experimental frequencies and modes, whereas, the
407 RFM minimizes the difference between analytical and experimental frequency
408 response functions.

409 Figure 11 shows the damage detected in each case (the cases are defined in

410 section 3.1). In cases 1 and 2 the real damage is detected by the three methods.
411 In case 3 only the GA and IESM methods detect the real damage. In case 4 only
412 the GA method detects the damage. As the differences between the damage
413 and undamaged models become higher, the optimization problem becomes
414 unstable and it becomes impossible to reach the optimum solution. On the
415 other hand, the genetic algorithm method is unaffected by these differences,
416 and the optimum solution is always reached as is shown in Figure 11. False
417 damage is detected always with both the IESM and RFM methods; the latter
418 detects a higher quantity.

419 Figure 12 illustrates the correlation in frequency and modes before and after
420 damage detection. The correlation in frequency is expressed as the relative fre-
421 quency difference between the numerical and experimental frequencies. The
422 correlation between the numerical and experimental modes is determined with
423 the MAC values. When the numerical model is updated with the damage de-
424 tected a significant improvement in the correlation is reached. The differences
425 in frequencies after updating are lower than 10% in all cases. And the MAC
426 values after updating are always higher than 75%.

427 5.1 *Incomplete Degrees of Freedom*

428 To define the number of degrees of freedom (DOF) necessary to detect the
429 damage, the method was evaluated with several levels of incompleteness in the
430 measured data. A total of 4 to 32 DOF are considered, these corresponds to 0.9
431 to 7.2 percent of the total DOF in the numerical model. The locations with a
432 higher sensitivity to damage were chosen as measuring points. To do these, the
433 mode shapes sensitivities were evaluated for each mode shape in all possible

434 damage locations. Then, the first n points with the higher average sensitivity
435 were chosen. The average sensitivity obtained for each DOF is shown in Figure
436 13. To visualize the most sensitive points in the structure, Figure 14 presents
437 the optimum set of measuring points with 8, 16 and 32 DOF.

438 Table 1 summarize the damage detected in each case. In the single damage
439 cases, it was possible to locate and quantify correctly the damage measuring
440 only 8 DOF (1.8% of the total DOF). When the number of damage locations
441 increases, the method requires a higher number of measured DOF. For two
442 simultaneous damages the method needs at least 12 DOF (2.7% of the total
443 DOF), and three simultaneous damages locations require at least 28 DOF
444 (6.3% of the total DOF). This indicates that the number of DOF required,
445 depends on the structure and the complexity of the damage situation that
446 needs to be detected.

447 6 Conclusions

448 A hybrid real-coded genetic algorithm has been implemented to detect struc-
449 tural damage. A damage penalization term is added to the objective function
450 to avoid false damage detection caused by experimental noise or numerical er-
451 rors. The algorithm is verified on a tridimensional space frame structure with
452 single and multiple damage scenarios. In addition, the method is tested with
453 different levels of incompleteness in the measured degrees of freedom.

454 The results show that this Genetic Algorithm approach reaches a more precise
455 solution than conventional optimization methods. Real damage is successfully
456 detected and false damage detection is avoided, even in cases of large or com-

457 plex damage scenarios on which conventional optimization approaches fail to
458 reach the global optimum. A scenario of three simultaneous damage locations
459 was correctly located and quantified by measuring only 6.3% of the total de-
460 grees of freedom.

References

- [1] E. Carden, P. Fanning, Vibration Based Condition Monitoring: A Review, *Structural Health Monitoring* 3 (4) (2004) 355–377.
- [2] O. Salawu, Detection of structural damage through changes in frequency: a review, *Engineering Structures* 19 (9) (1997) 718–723.
- [3] Z. Shi, S. Law, L. Zhang, Damage Localization by Directly Using Incomplete Mode Shapes, *Journal of Engineering Mechanics* 126 (6) (2000) 656–660.
- [4] J. Araújo dos Santos, C. Soares, C. Mota Soares, H. Pina, A damage identification numerical model based on the sensitivity of orthogonality conditions and least squares techniques, *Computers and Structures* 78 (1-3) (2000) 283–291.
- [5] W. Ren, G. De Roeck, Structural Damage Identification using Modal Data. I: Simulation Verification, *Journal of Structural Engineering* 128 (2002) 87–95.
- [6] W. Ren, G. De Roeck, Structural Damage Identification using Modal Data. II: Test Verification, *Journal of Structural Engineering* 128 (2002) 96–104.
- [7] M. M. Abdel Wahab, Effect of modal curvatures on damage detection using model updating, *Mechanical Systems and Signal Processing* 15 (2) (2001) 439–445.

- [8] E. Görl, M. Link, Damage identification using changes of eigenfrequencies and mode shapes, *Mechanical Systems and Signal Processing* 17 (1) (2003) 103–110.
- [9] B. Jaishi, W. Ren, Finite element model updating based on eigenvalue and strain energy residuals using multiobjective optimization technique, *Mechanical Systems and Signal Processing* 21 (5) (2007) 2295–2317.
- [10] B. Jaishi, W. Ren, Damage detection by finite element model updating using modal flexibility residual, *Journal of Sound and Vibration* 290 (1-2) (2006) 369–387.
- [11] J. Kosmatka, J. Ricles, Damage Detection in Structures by Modal Vibration Characterization, *Journal of Structural Engineering* 125 (1999) 1384–1392.
- [12] Z. Wang, R. Lin, M. Lim, Structural damage detection using measured FRF data, *Computer Methods in Applied Mechanics and Engineering* 147 (1-2) (1997) 187–197.
- [13] M. Imregun, W. Visser, D. Ewins, Finite element model updating using frequency response function data I. Theory and initial investigation, *Mechanical Systems and Signal Processing* 9 (2) (1995) 187–202.
- [14] S. Lammens, Frequency response based validation of dynamic structural finite element models, Leuven, 1995.
- [15] H. Natke, Problems of model updating procedures: A perspective resumption, *Mechanical Systems and Signal Processing* 12 (1) (1998) 65–74.
- [16] M. Zehn, O. Martin, R. Onger, Influence of Parameter Estimation Procedures on the Updating Process of Large Finite Element Models, Proceedings of the 2nd International Conference on Identification in Engineering Systems, Swansea, UK, 1999 March.
- [17] M. Srinivas, L. Patnaik, Genetic algorithms: a survey, *Computer* 27 (6)

- (1994) 17–26.
- [18] J. Holland, *Adaptation in natural and artificial systems*, University of Michigan Press Ann Arbor, 1975.
- [19] J. Joines, C. Houck, On the use of non-stationary penalty functions to solve nonlinear constrained optimization problems with GA's, in: *IEEE International Symposium Evolutionary Computation*, Orlando, FL, USA, 1994, pp. 579–584.
- [20] B. Miller, D. Goldberg, Genetic algorithms, tournament selection, and the effects of noise, Tech. Rep. 95006, Department of General Engineering, University of Illinois at Urbana-Champaign (1995).
- [21] L. Eshelman, R. Caruana, J. Schaffer, Biases in the crossover landscape, in: *Proceedings of the third international conference on Genetic algorithms table of contents*, Morgan Kaufmann Publishers Inc. San Francisco, CA, USA, 1989, pp. 10–19.
- [22] G. Syswerda, Uniform crossover in genetic algorithms, in: *Proceedings of the 3rd International Conference on Genetic Algorithms table of contents*, Morgan Kaufmann Publishers Inc. San Francisco, CA, USA, 1989, pp. 2–9.
- [23] N. Radcliffe, Forma analysis and random respectful recombination, in: *Proceedings of the Fourth International Conference on Genetic Algorithms*, 1991, pp. 222–229.
- [24] Z. Michalewicz, *Genetic Algorithms+ Data Structures= Evolution Programs*, Springer, 1996.
- [25] A. Wright, Genetic algorithms for real parameter optimization, *Foundations of Genetic Algorithms 1* (1991) 205–218.
- [26] L. Eshelman, J. Schaffer, Real-coded genetic algorithms and interval-schemata, in: *Foundations of Genetic Algorithms 2*, Vol. 21, San Mateo,

- 1993, pp. 187–202.
- [27] H. M. Elkamchouchi, M. Wagih, Genetic algorithm operators effect in optimizing the antenna array pattern synthesis, in: Proceedings of the 20th National Radio Science Conference, Cairo, Egypt, 2003.
- [28] C. Mares, C. Surace, An application of genetic algorithms to identify damage in elastic structures, *Journal of Sound and Vibration* 195 (2) (1996) 195–215.
- [29] M. Rao, J. Srinivas, B. Murthy, Damage detection in vibrating bodies using genetic algorithms, *Computers and Structures* 82 (11-12) (2004) 963–968.
- [30] R. Ruotolo, C. Surace, Damage assessment of multiple cracked beams: numerical and experimental validation, *Journal of Sound and Vibration* 206 (4) (1997) 567–588.
- [31] M. Friswell, J. Penny, S. Garvey, A combined genetic and eigensensitivity algorithm for the location of damage in structures, *Computers and Structures* 69 (5) (1998) 547–556.
- [32] C. Koh, Y. Chen, C. Liaw, A hybrid computational strategy for identification of structural parameters, *Computers and Structures* 81 (2) (2003) 107–117.
- [33] R. Perera, A. Ruiz, C. Manzano, Performance assessment of multicriteria damage identification genetic algorithms, *Computers & Structures* 87 (1-2) (2009) 120 – 127.
- [34] H. Asce, Y. Xia, Vibration-based damage detection of structures by genetic algorithm, *Journal of Computing in Civil Engineering* 16 (2002) 222.
- [35] R. He, S. Hwang, Damage detection by an adaptive real-parameter simulated annealing genetic algorithm, *Computers and Structures* 84 (31-32)

- (2006) 2231–2243.
- [36] M. Vakil-Baghmisheh, M. Peimani, M. Sadeghi, M. Ettefagh, Crack detection in beam-like structures using genetic algorithms, *Applied Soft Computing Journal*.
- [37] H. Gomes, N. Silva, Some comparisons for damage detection on structures using genetic algorithms and modal sensitivity method, *Applied Mathematical Modelling* 32 (11) (2008) 2216–2232.
- [38] R. Haupt, S. Haupt, *Practical Genetic Algorithms*, Wiley-Interscience, 2004.
- [39] Y. Yan, L. Cheng, Z. Wu, L. Yam, Development in vibration-based structural damage detection technique, *Mechanical Systems and Signal Processing* 21 (5) (2007) 2198–2211.
- [40] C. Borges, H. Barbosa, A. Lemonge, A structural damage identification method based on genetic algorithm and vibrational data, *International Journal for Numerical Methods in Engineering* 69 (2007) 2663–2686.
- [41] B. Kouchmeshky, W. Aquino, J. Bongard, H. Lipson, Co-evolutionary algorithm for structural damage identification using minimal physical testing, *International Journal for Numerical Methods in Engineering* 69 (5) (2007) 1085–1107.
- [42] B. Kouchmeshky, W. Aquino, A. Billek, Structural damage identification using co-evolution and frequency response functions, *Structural Control and Health Monitoring* 15 (2) (2008) 162–182.
- [43] F. Au, Y. Cheng, L. Tham, Z. Bai, Structural damage detection based on a micro-genetic algorithm using incomplete and noisy modal test data, *Journal of Sound and Vibration* 259 (5) (2003) 1081–1094.
- [44] A. Raich, T. Liskai, Improving the performance of structural damage detection methods using advanced genetic algorithms, *Journal of Structural*

- Engineering 133 (2007) 449–461.
- [45] Y. Xia, H. Hao, J. Brownjohn, P. Xia, Damage identification of structures with uncertain frequency and mode shape data, *Earthquake Engineering and Structural Dynamics* 31 (2002) 1053–1066.
- [46] M. Friswell, J. Penny, Crack modeling for structural health monitoring, *Structural Health Monitoring* 1 (2) (2002) 139–148.
- [47] R. J. Allemang, D. L. Brown, A correlation coefficient for modal vector analysis, in: *Proceedings of the First International Modal Analysis Conference*, Orlando, Florida, 1982, pp. 110–116.
- [48] R. Guyan, Reduction of mass and stiffness matrices, *AIAA Journal* 3 (2) (1965) 380.
- [49] T. Breitfeld, A method for identification of a set of optimal measurement points for experimental modal analysis, in: *Proceedings of the 13th International Modal Analysis Conference*, Nashville, United States, 1995, pp. 1029–1034.
- [50] D. Kientzy, M. Richardson, K. Blakely, Using finite element data to set up modal tests, *Sound and Vibration Magazine* 23 (1989) 16–23.
- [51] S. Modak, T. Kundra, B. Nakra, Comparative Study of Model Updating Methods Using Simulated Experimental Data, *Computers and Structures* 80 (5-6) (2002) 437–447.

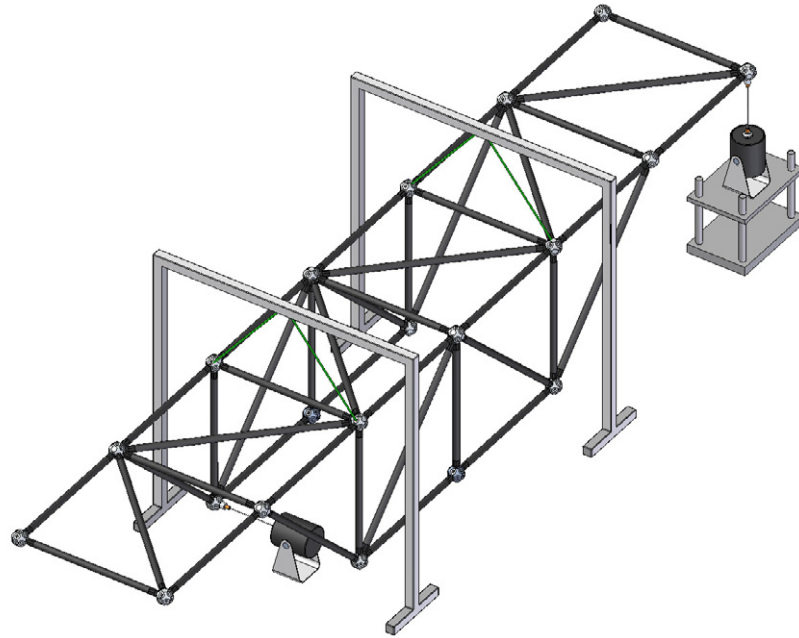


Fig. 1. Experimental Setup

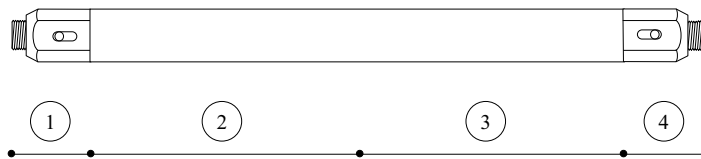


Fig. 2. FE model of each bar

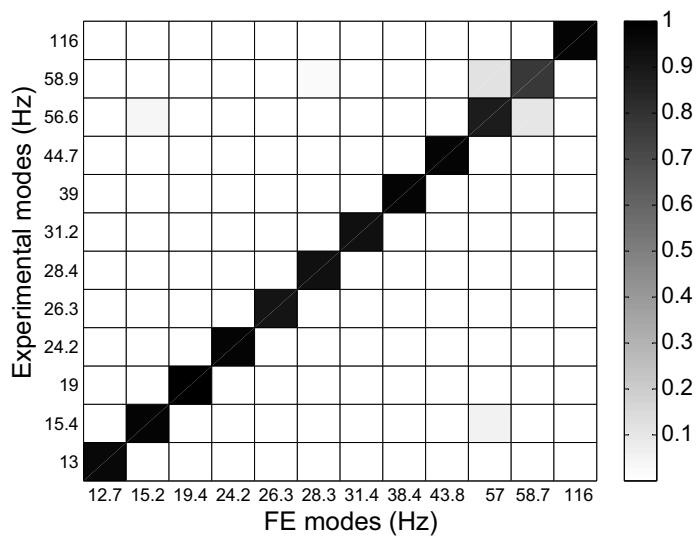


Fig. 3. Initial MAC

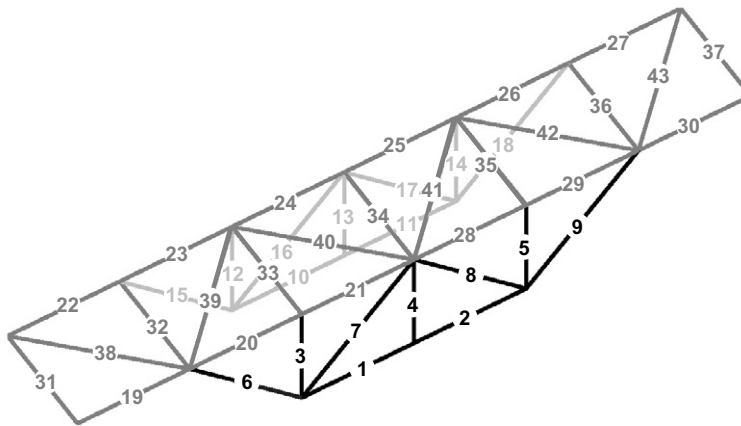


Fig. 4. Bar numbering

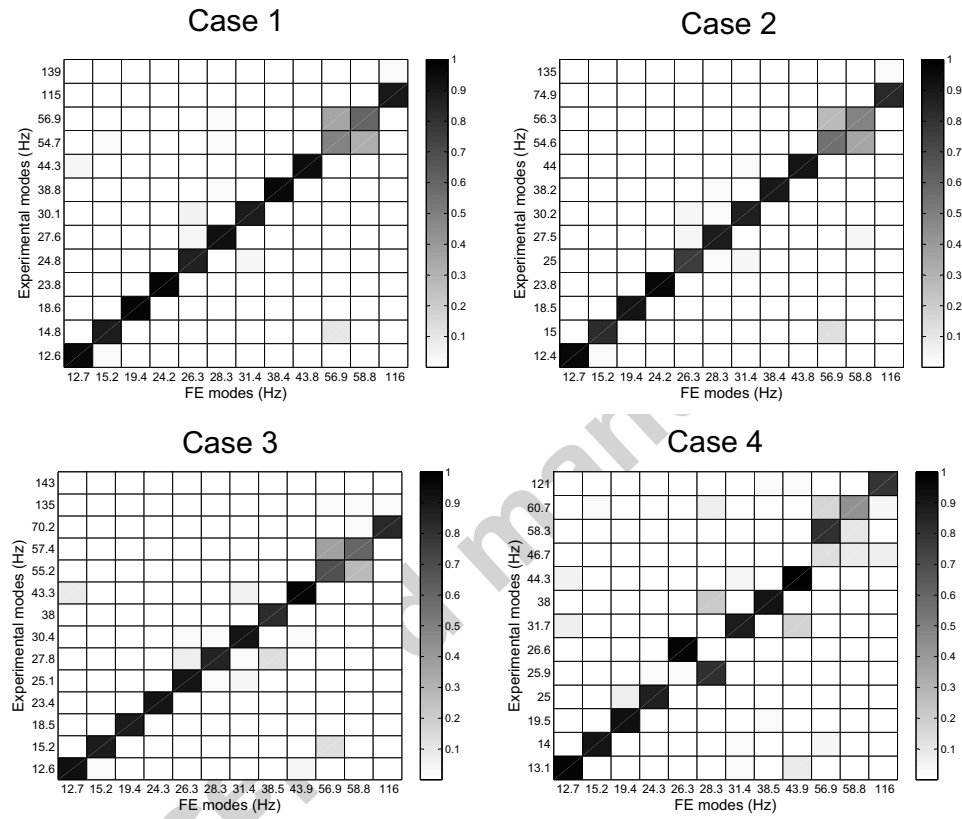


Fig. 5. Correlation between the undamaged numerical and damaged experimental modes

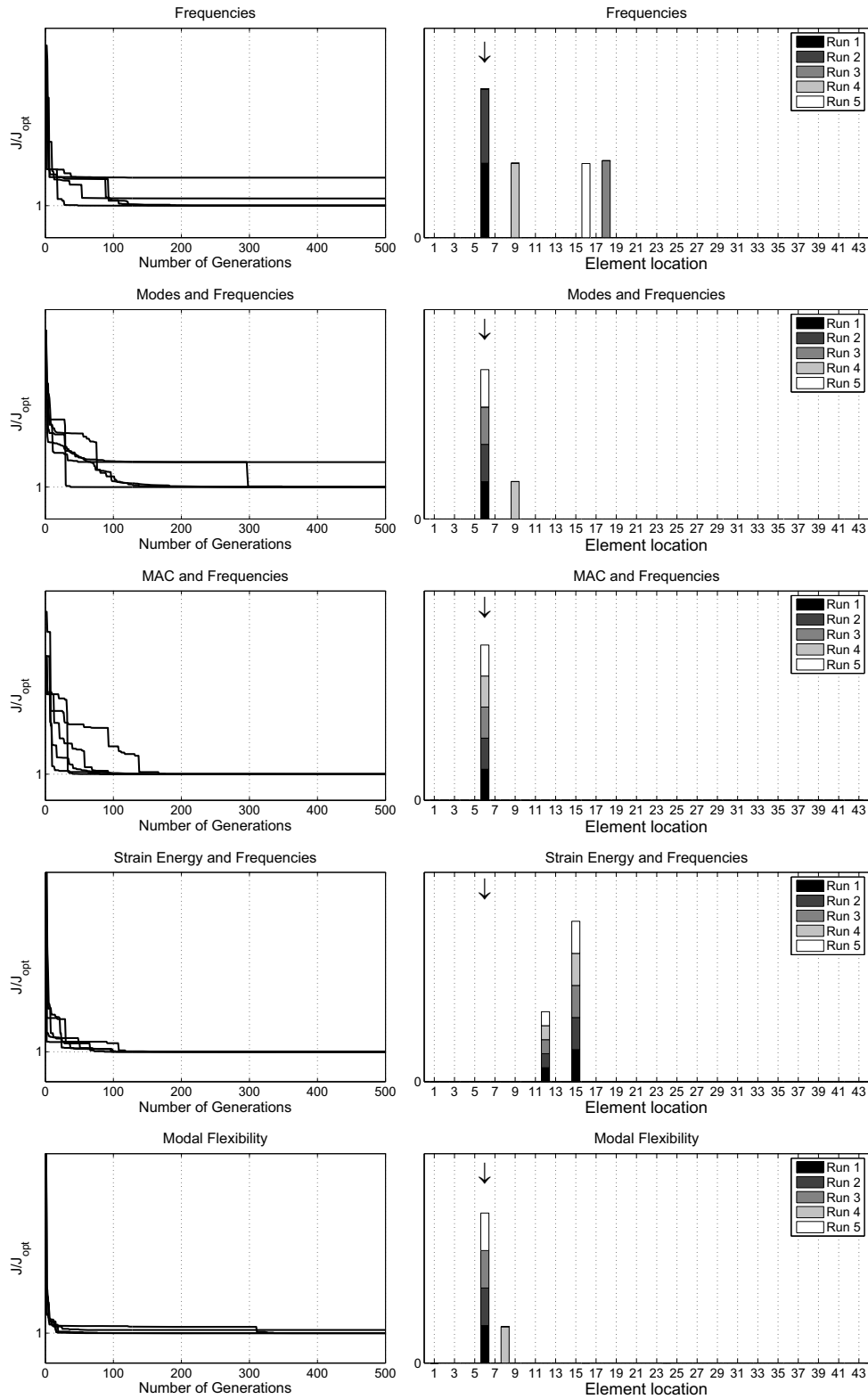


Fig. 6. Convergence curve and solution of different objective functions based on modal data

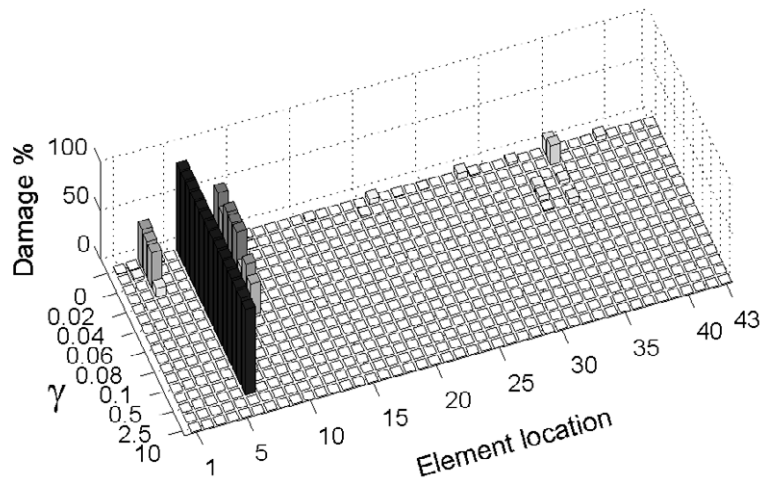


Fig. 7. Effect of on the damage detected

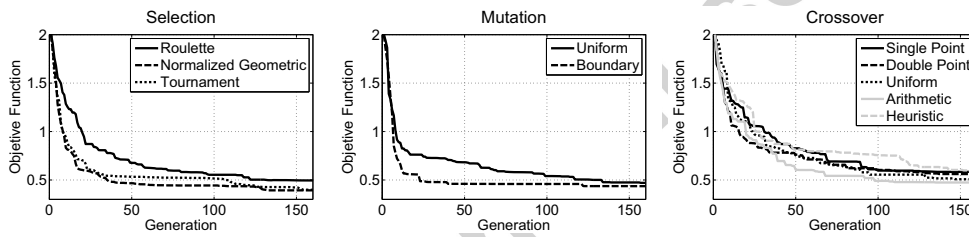


Fig. 8. Average convergence curves after running 20 times for different: left - selection processes, middle - mutation operators and right - crossover operators

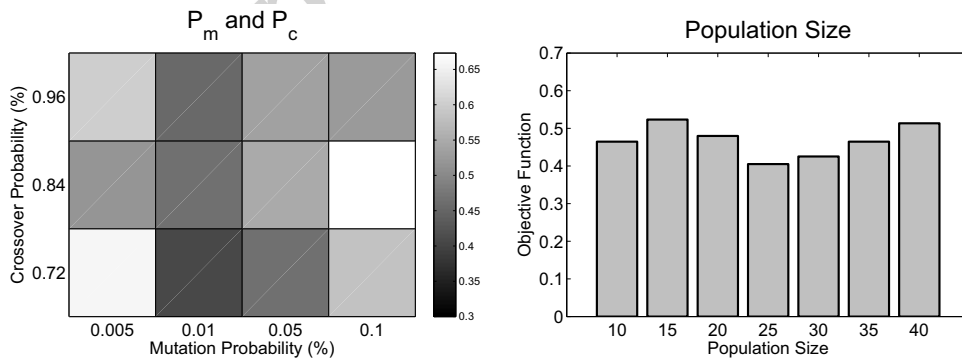


Fig. 9. Average value of the objective function after running 20 times for different combinations of crossover and mutation probabilities (left) and for different population sizes (right)

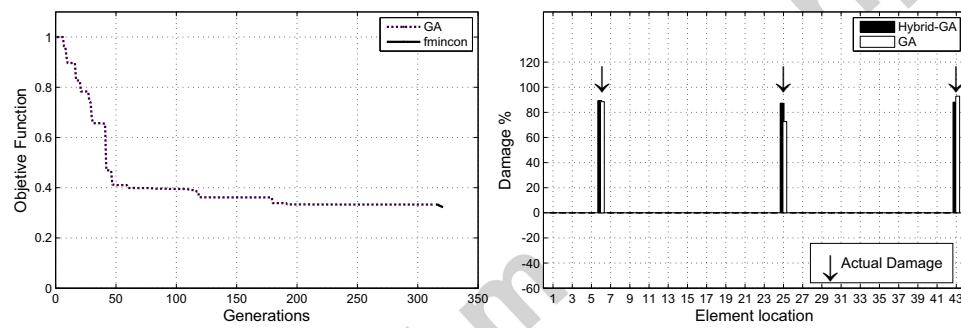


Fig. 10. Right: Curve of converge of the GA followed by a local optimizer. Left: Damage detected with GA and with a hybrid-GA

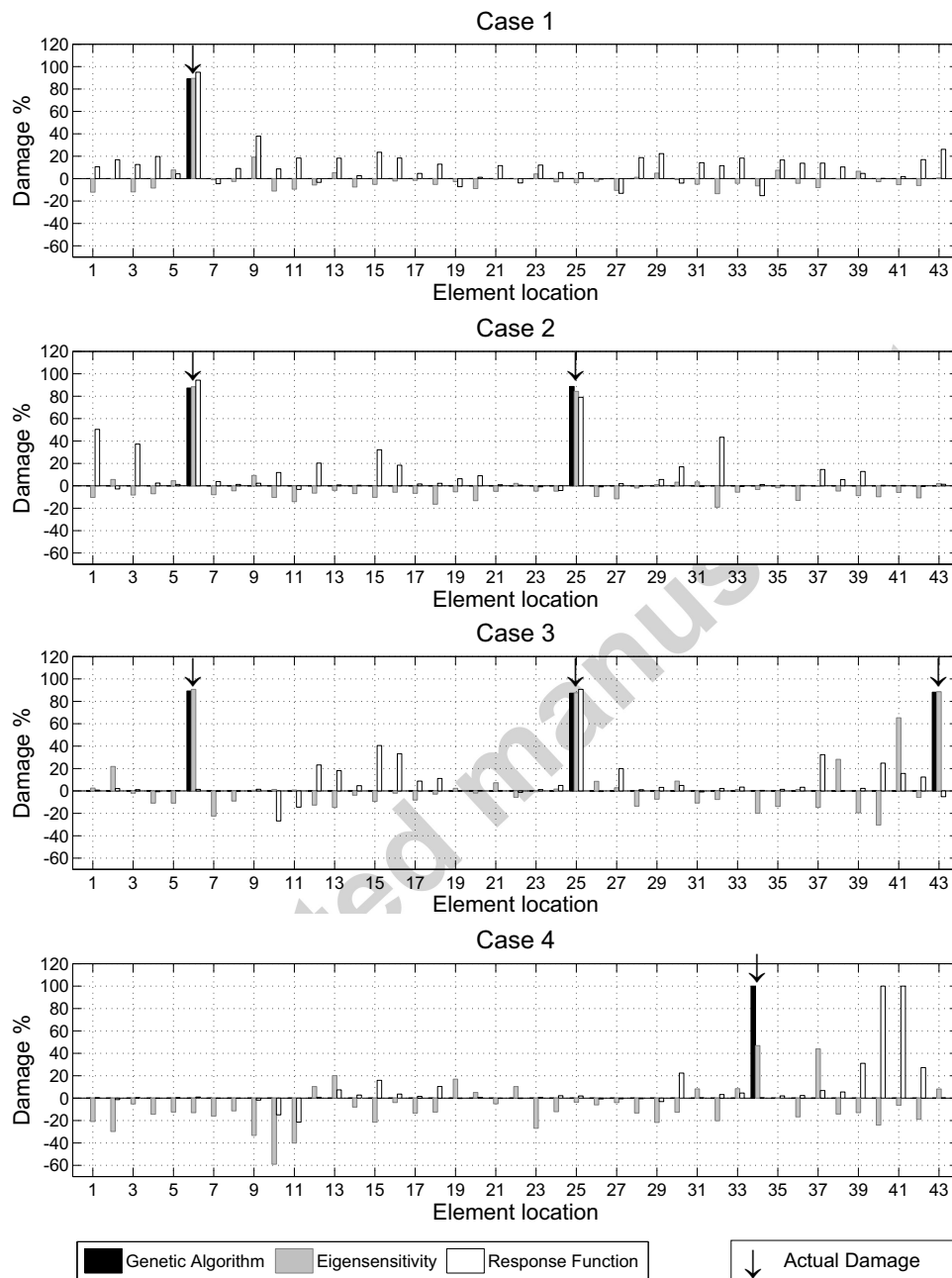


Fig. 11. Damage detected with the proposed algorithm compared to two classical damage detection methods

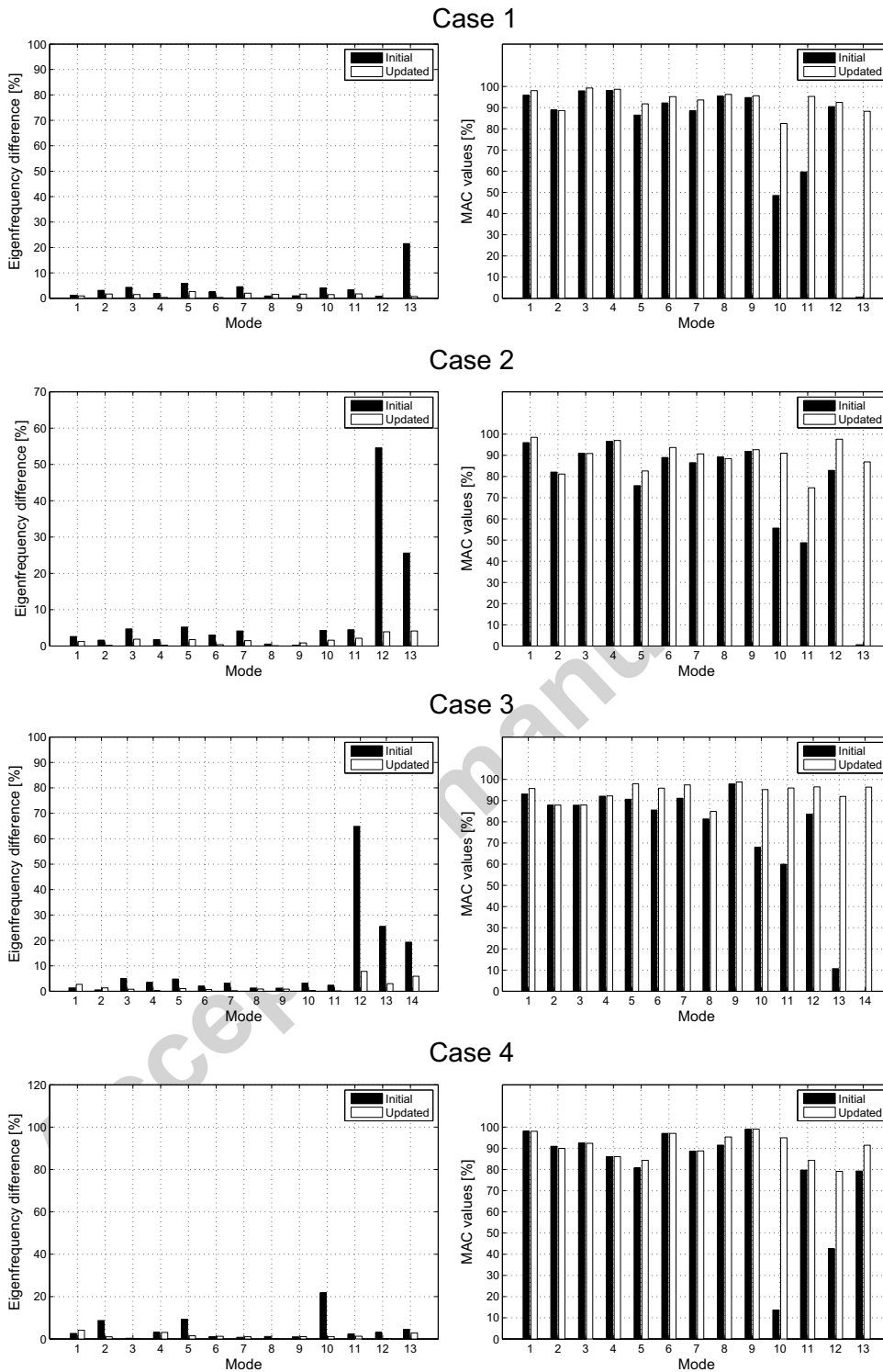


Fig. 12. Improvement in the correlation in frequency and modes after damage detection

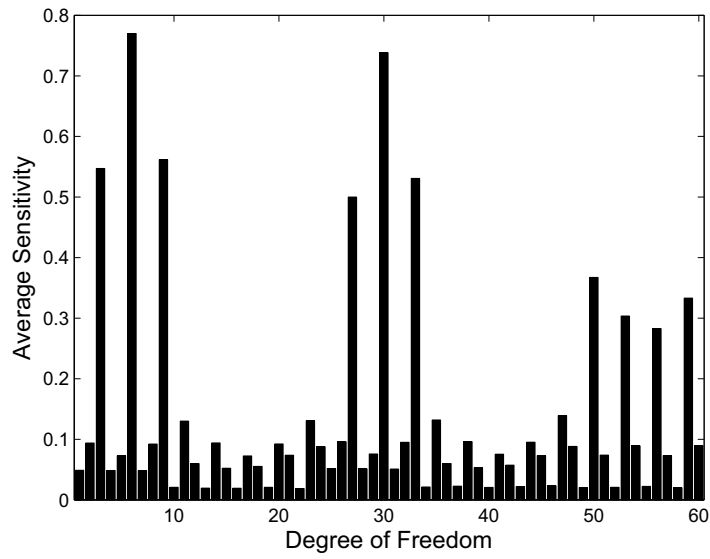


Fig. 13. Average sensitivity to damage for each DOF

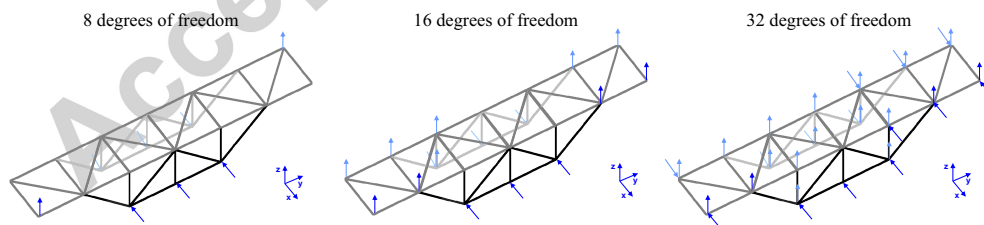


Fig. 14. Optimum set of measuring points

Case	N of measured DOF	Real		Detected	
		Location	Damage %	Location	Damage %
1	4	6	92	3,22	95,21
	6	6	92	3,6	51,93
	8	6	92	6	92
	12	6	92	6	92
	16	6	92	6	92
4	4	34	100	26,34,43	13,100,7
	6	34	100	6,26,34,43	2,19,100,1
	8	34	100	34	100
	12	34	100	34	100
	16	34	100	34	100
2	8	6,25	92,92	6,26	92,92
	12	6,25	92,92	6,25	91,91
	16	6,25	92,92	6,25	92,91
	20	6,25	92,92	6,25	92,91
	24	6,25	92,92	6,25	92,92
3	12	6,25,43	92,92,92	6,42	89,94
	16	6,25,43	92,92,92	6,25,43	89,89,90
	20	6,25,43	92,92,92	6,25,26	89,90,90
	24	6,25,43	92,92,92	6,25,42	89,86,92
	28	6,25,43	92,92,92	6,25,43	89,90,90
	32	6,25,43	92,92,92	6,25,43	89,90,89

Table 1
Damage detected with different number of measured DOF